A Predictive Model of the Temperature-Dependent Inactivation of Coronaviruses

- 2 Te Faye Yap, a Zhen Liu, a,† Rachel A. Shveda, a,† Daniel J. Prestona,*

- ^aDepartment of Mechanical Engineering, Rice University, 6100 Main St., Houston, TX 77006, USA
- [†]Denotes equal contribution
- 7 *To whom correspondence should be addressed: dip@rice.edu

ABSTRACT

The COVID-19 pandemic has stressed healthcare systems and supply lines, forcing medical doctors to risk infection by decontaminating and reusing single-use personal protective equipment. The uncertain future of the pandemic is compounded by limited data on the ability of the responsible virus, SARS-CoV-2, to survive across various climates, preventing epidemiologists from accurately modeling its spread. However, a detailed thermodynamic analysis of experimental data on the inactivation of SARS-CoV-2 and related coronaviruses can enable a fundamental understanding of their thermal degradation that will help model the COVID-19 pandemic and mitigate future outbreaks. This work introduces a thermodynamic model that synthesizes existing data into an analytical framework built on first principles, including a first-order reaction rate law and the Arrhenius equation, to accurately predict the temperature-dependent inactivation of coronaviruses. The model provides much-needed thermal decontamination guidelines for personal protective equipment, including masks. For example, at 70 °C, a 3-log (99.9%) reduction in virus concentration can be achieved, on average, in 3 minutes (under the same conditions, a more conservative decontamination time of 39 minutes represents the upper limit of 95% prediction interval) and can be performed in most home ovens without reducing the efficacy of typical N95 masks as shown in recent experimental reports. This model will also allow for epidemiologists to incorporate the lifetime of SARS-

- 25 CoV-2 as a continuous function of environmental temperature into models forecasting the spread of the
- pandemic across different climates and seasons.

MAIN TEXT

The COVID-19 pandemic has overwhelmed medical facilities worldwide and caused a shortage of typically-disposable personal protective equipment (PPE), forcing medical workers to reuse or work without proper PPE.^{1,2} Researchers have explored decontamination procedures that might allow PPE to be reused safely,^{3,4} and medical workers have begun implementing these procedures, including decontaminating disposable masks with ultraviolet (UV) irradiation.⁵ However, UV decontamination faces several drawbacks, including an inability to kill viruses trapped within crevices that are not illuminated and a lack of availability at clinics in low-income areas and in most peoples' homes.⁶ Alternative methods of decontamination, namely steam sterilization, alcohol washing, and bleach washing, are useful for glassware and other durable materials, but have been reported to degrade single-use PPE.^{4,7,8} On the other hand, dry heat decontamination can be performed almost anywhere (including home ovens and rice cookers) and inactivates viruses within crevices without damaging delicate PPE.^{7,9,10} However, dry heat decontamination guidelines for SARS-CoV-2 remain limited to a few experimental measurements constrained to specific temperatures that do not apply to all heating devices.¹¹

Meanwhile, virus transmission has been linked to variations in outdoor climate, where colder atmospheric temperatures lead to longer virus lifetimes outside of hosts. This effect has been reported for influenza, 12,13 the common cold, 14 SARS-CoV-2, 11,15 SARS-CoV-1, 16,17 and MERS-CoV. 18,19 Even at a local scale, a recent resurgence of COVID-19 cases in a seafood market was linked to low temperatures. 20 Epidemiologists would benefit from knowledge of the lifespan of SARS-CoV-2 as a continuous function of atmospheric temperature to accurately model the spread of COVID-19. Furthermore, understanding the temperature-dictated inactivation time could help predict the resurgence of cases as colder weather returns to the Northern Hemisphere, following a similar trend to that of the seasonal flu. 21

We introduce an analytical model based on a first-order reaction rate law and Arrhenius equation that enables prediction of the thermal inactivation rate and lifetime of coronaviruses, including SARS-CoV-2, as a function of temperature. These viruses are treated as macromolecules undergoing thermal denaturation; we confirm that coronaviruses undergo thermal denaturation because their inactivation behavior follows the Meyer-Neldel rule.²² The time required to achieve a desired log-scale reduction in viable virions (e.g. by a factor of 10³ as typically used for viral decontamination^{23–26}) was used to generate dry heat decontamination guidelines for SARS-CoV-2 relevant to temperature ranges accessible in commonly-available heating devices. The model also predicts the lifetime of human coronaviruses as a continuous function of temperature in various climates, which will assist epidemiologists in understanding the regionally-dependent lifetime of the SARS-CoV-2 virus as well as the potential of a COVID-19 resurgence in autumn and winter.

Reports in literature provide abundant data to construct a predictive analytical model capturing the thermal effects on virus inactivation. We focused specifically on the inactivation of coronaviruses, a group of enveloped viruses often responsible for respiratory or gastrointestinal diseases in mammals and birds.²⁷ We compiled hundreds of data points for inactivation of five coronaviruses, with subdivisions based on (i) strains of each virus, (ii) environmental pH levels, and (iii) relative humidity conditions, resulting in fourteen datasets (**Figure 1(a)**). These viruses include: (i) Severe Acute Respiratory Syndrome Coronavirus (SARS CoV-1 and SARS-CoV-2);^{11,17,28-30} (ii) Middle East Respiratory Syndrome Coronavirus (MERS-CoV);^{18,19} (iii) Transmissible Gastroenteritis Virus (TGEV);³¹ (iv) Mouse Hepatitis Virus (MHV);^{32,33} and (v) Porcine Epidemic Diarrhea Virus (PEDV).³⁴

The rate law describes the inactivation behavior of microbes.³⁵ Non-first-order rate laws have been applied to inactivation of some microbes,^{36–38} particularly bacteria with heterogeneous populations,³⁹ but the inactivation of most viruses—including the coronaviruses considered in our analysis—follow a first-order reaction, with viable virions as reactants and inactivated virions as products (Eq. 1):

$$[C] = [C_0]e^{-kt}, (Eq. 1)$$

The majority of primary experimental data for the inactivation of viruses is reported in plots of the log of concentration $\ln([C])$ as a function of time, t, with C_0 being the initial concentration of viable virions. We applied a linear regression to each set of primary data to determine the rate constant, k, for inactivation of a virus at a given temperature, T, determined by calculating the slope, $k = -\Delta \ln([C])/\Delta t$. Each of these pairs of (k, T) yields one data point in **Figure 1(a)**, with details in the supplementary material, **Figures S1–S28**.

Virus inactivation occurs due to thermal denaturation of the proteins that comprise each virion. The temperature dependence of the thermal denaturation process is captured by the Arrhenius equation, 40 which yields a linear relationship between ln(k) and 1/T (Eq. 2):

$$\ln(k) = -\frac{E_a}{RT} + \ln(A), \tag{Eq. 2}$$

where R is the gas constant, E_a is the activation energy associated with inactivation of the virus (i.e., the energy barrier to be overcome for protein denaturation), and A is the frequency factor. In **Figure 1(a)**, the $\ln(k)$ and 1/T are plotted according to the Arrhenius equation (Eq.2). The activation energy, E_a , and natural log of the frequency factor, $\ln(A)$, can be obtained by equating $-E_a/R$ and $\ln(A)$ from Eq. 2 with the slopes and intercepts from the linear fits in **Figure 1(a)**, respectively, and plotted in **Figure 1(b)**. The linear correlation between $\ln(A)$ and E_a indicates that coronaviruses undergo a thermal denaturation process following the Meyer-Neldel rule, ²² supporting our hypothesis that they are inactivated primarily by thermally-driven

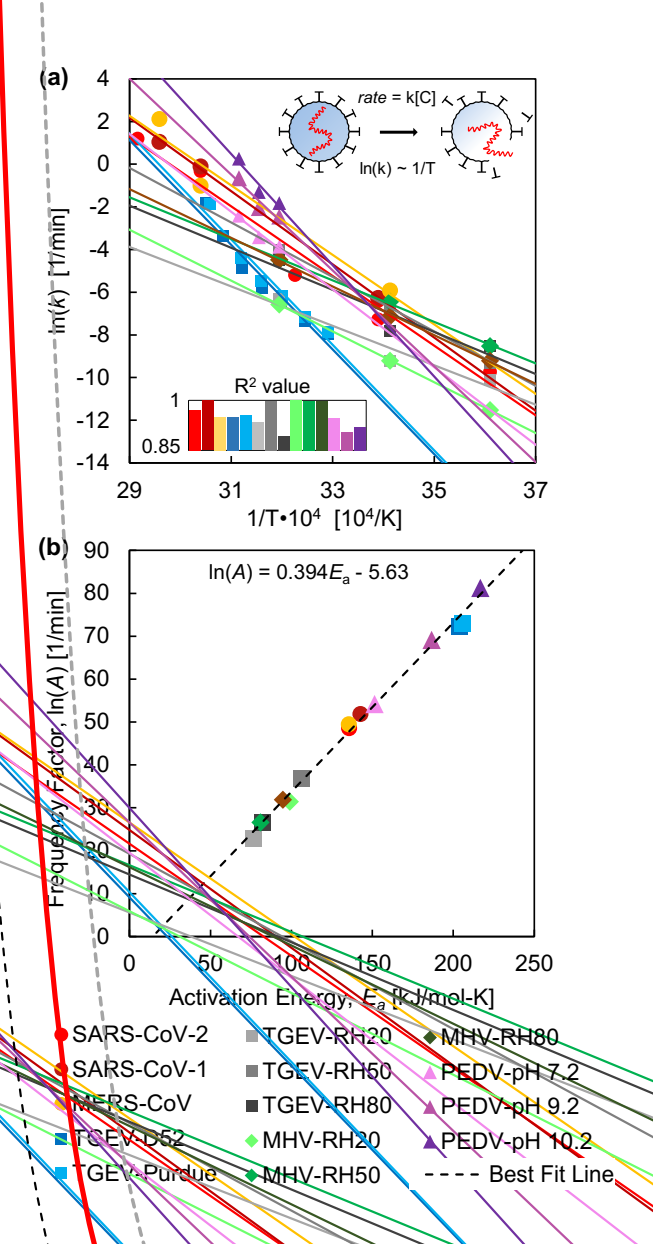


Figure 1 (Single Column). Thermal inactivation behavior of coronaviruses. An Arrhenius plot (a) shows the dependence of inactivation rate constant on temperature for the coronaviruses. Each coronavirus dataset was fitted using linear regression (Eq. 2), where the inserted chart presents the R^2 values for the linear fits. The resulting activation energy, E_a , and frequency factor, ln(A), were back-calculated from each

linear fit according to Eq. 2 and plotted (b); the linear correlation between ln(A) and E_a indicates protein

denaturation. ^{22,41}

degradation of proteins. In fact, the linear regression calculated in this work, $[\ln(A) = 0.394E_a - 5.63]$, is nearly identical to those calculated in two prior studies on the denaturation of tissues and cells, which report $[\ln(A) = 0.380E_a - 5.27]^{22}$ and $[\ln(A) = 0.383E_a - 5.95]$.

The degree of inactivation of a pathogen is defined by the ratio of the concentration (amount) of a pathogen to its initial concentration, $[C]/[C_0]$, often in terms of orders of magnitude; an n-log inactivation refers to a reduction in concentration of 10 raised to the nth power ($[C]/[C_0] = 10^{-n}$). Equations 1 and 2 combine to yield an analytical model used in determining the time required to achieve an n-log reduction in a pathogen (Eq. 3):

$$t_{n-log} = -\frac{1}{A}e^{\left(\frac{E_a}{RT}\right)}\ln(10^{-n}),$$
 (Eq. 3)

The US Food and Drug Administration recommends a 3-log (99.9%) reduction in number of virions for decontamination of non-enveloped viruses (i.e. $[C]/[C_0] = 10^{-3}$). Since non-enveloped viruses are shown to be more resilient to elevated environmental temperatures than their enveloped counterparts (including coronaviruses), we refer to the time required to achieve a 3-log reduction as the coronavirus *lifetime*, indicative of a conservative prediction for both decontamination time and viable lifetime outside a host. The time required to achieve an *n*-log reduction is directly proportional to the *n* value; therefore, a more conservative decontamination time could be obtained by inserting a different value of *n* into Eq. 3, which would change the *n*-log reduction predictions by a multiplicative factor of $n_{desired}/n_{current}$, (e.g. in this work, $n_{current} = 3$; therefore, a 6-log reduction would require doubling of the times predicted in this work). **Figure 2** reports the virus lifetimes generated from Eq. 3 as a function of temperatures ranging from room temperature to temperatures achievable using common heating devices. In **Figure 2(a)**, all five types of

coronaviruses are plotted to show the variation across different environmental temperatures. The plot in **Figure 2(b)** shows similar data, with the exception of data from Casanova, et al., due to possible experimental error in the primary data (see supplementary material, Section S3), and

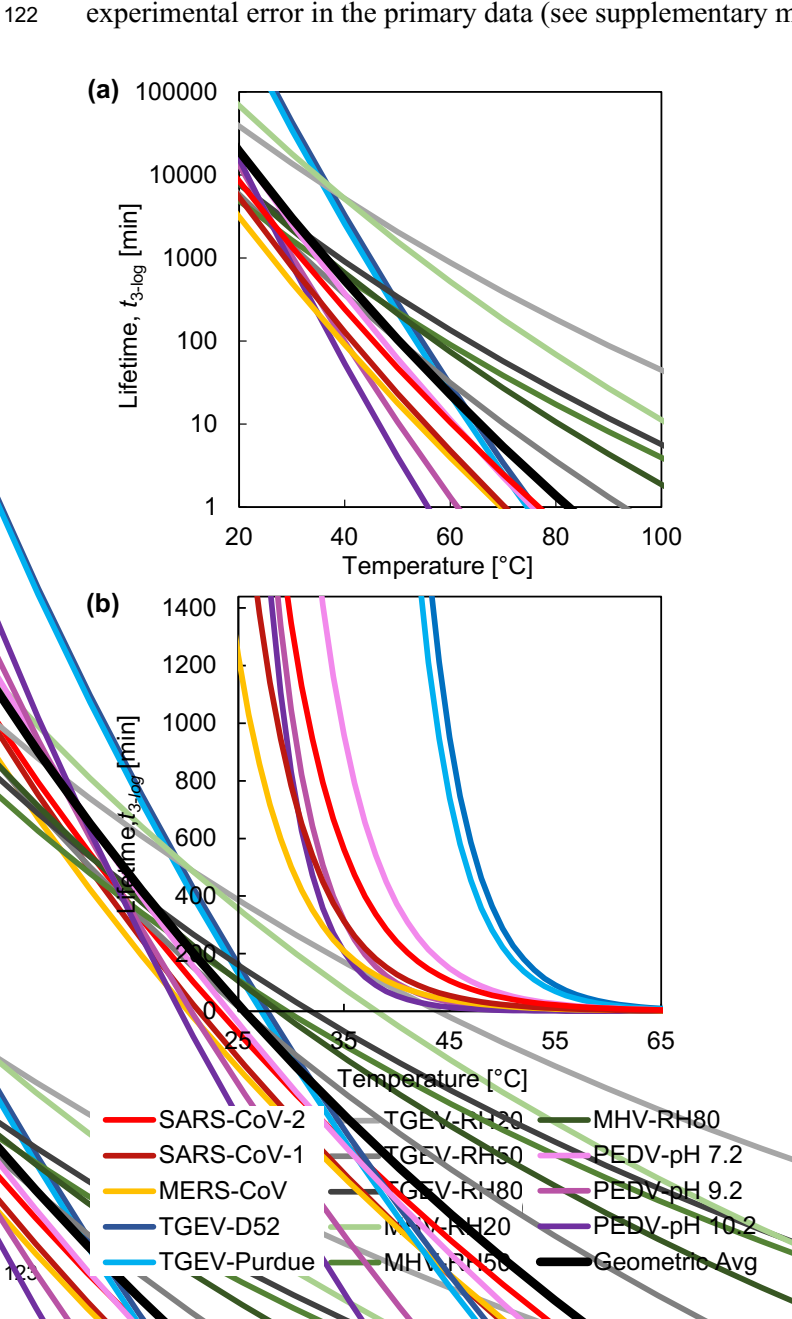


Figure 2 (Single Column). Virus lifetime as a function of temperature. Predictions are shown in (a) for all the coronaviruses analyzed in this work, with the average lifetime presented in black. All coronaviruses

excluding data sourced from Casanova, et al., are replotted in (b) with a linearly-scaled vertical axis (1440 minutes = 1 day) to highlight the exponential dependence of lifetime on temperature.

128

129

130

131

132

133

134

135

136

137

138

139

140

141

142

143

144

126

127

with the lifetime axis scaled linearly to highlight the exponential dependence of lifetime on temperature. The human coronaviruses SARS-CoV-2 and SARS-CoV-1 exhibit a similar trend in thermal degradation, in agreement with recent work.³⁰ We observed that SARS-CoV-2 has a slightly longer mean lifetime than SARS-CoV-1 outside a host, potentially contributing to its relatively high reproduction number, R₀. However, based on uncertainty analysis, Figure 3 indicates that the prediction intervals of SARS-CoV-1 and SARS-CoV-2 overlap, suggesting that additional data would be needed to definitively support the conclusion that SARS-CoV-2 has a longer lifetime. The prediction interval is used to estimate variation in coronavirus lifetimes predicted by the analytical model. The prediction interval can account for uncertainties corresponding to different virus strains due to genetic mutations as well as variations in experimental conditions such as RH and fomites, and a conservative estimate of the maximum lifetime of a coronavirus given this uncertainty can be determined with different levels of confidence (90%, 95%, and 97.5% prediction intervals are shown in Figure 3). The details of statistical uncertainty for all of the viruses are included in the supplementary material, Table S3. The average lifetime for the human coronaviruses SARS-CoV-2 and SARS-CoV-1 are shown in Table I. The temperature values displayed in the table illustrate both (i) common environmental conditions and (ii) temperatures appropriate for thermal decontamination.

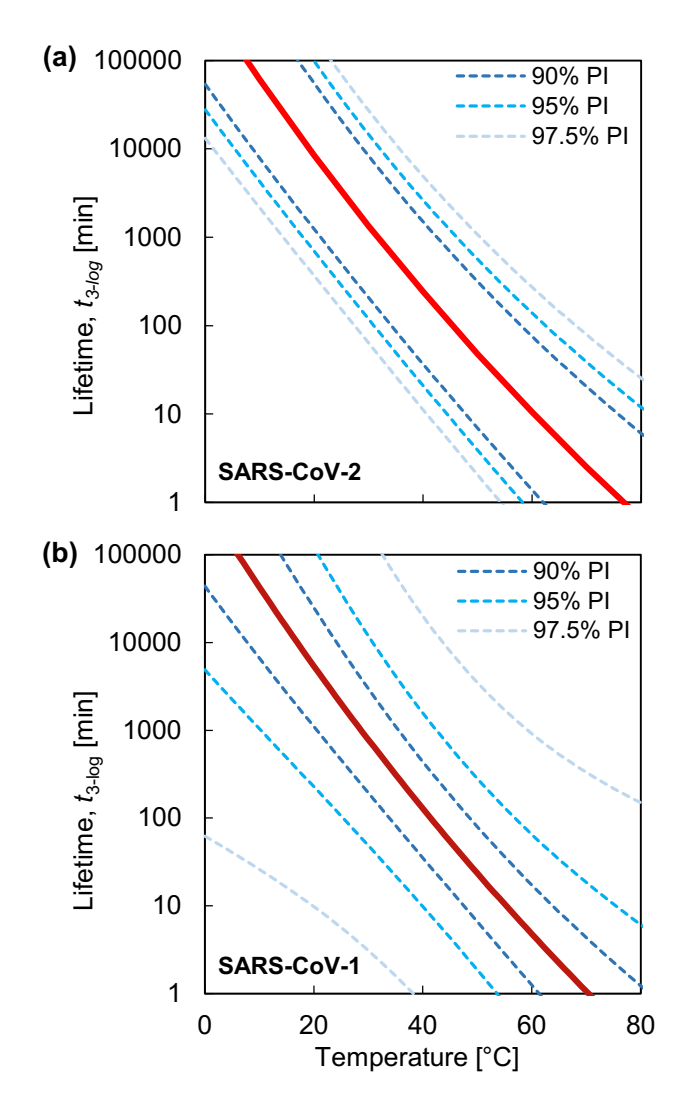


Figure 3 (Single Column). The lifetime of SARS-CoV-2 (a) and SARS-CoV-1 (b) are highlighted, and 90%, 95%, and 97.5% prediction intervals are used to illustrate uncertainties in the predicted lifetimes based on statistical analysis.

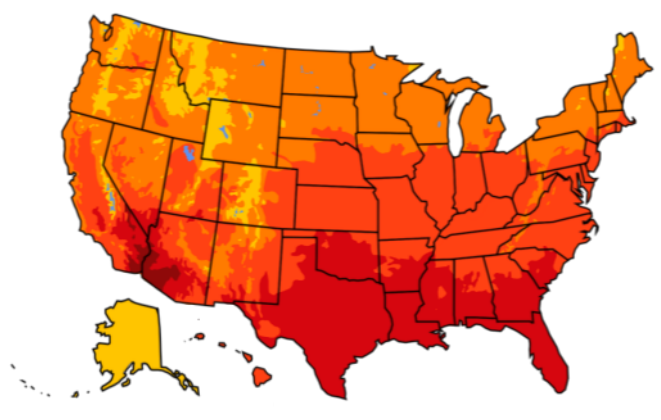
	Temperature	SARS-CoV-2 lifetime, t _{3-log}	SARS-CoV-1 lifetime, t _{3-log}
Environmental Conditions	10 °C	>1 month	29.8 d (> 1 month)
	15 °C	15.5 d (>1 month)	10.4 d (> 1 month)
	20 °C	5.9 d (>1 month)	3.8 d (> 1 month)
	25 °C	2.3 d (25.5 d)	1.4 d <i>(25.4 d)</i>
	30 °C	22.5 h (10 d)	13.1 h (8.26 d)
	35 °C	9.4 h (4.2 d)	5.2 h (2.9 d)
	40 °C	4.0 h (1.8 d)	2.1 h (1.1 d)
Deconta- mination	60 °C	10.5 min (2.3 h)	4.8 min (1.1 h)
	70 °C	2.5 min (38.6 min)	1.1 min (18.4 min)
	80 °C	< 1 min (11.9 min)	< 1 min (6.1 min)
	90 °C	< 1 min (4.0 min)	< 1 min (2.3 min)

We estimated the regional lifetime of SARS-CoV-2 based on climate temperatures in the United States. We used temperatures averaged over January to March, 2020, corresponding to the onset of the COVID-19 pandemic (Figure 4(a)), and July to September, 2019, as a rough prediction of SARS-CoV-2 lifetimes in summer 2020 (Figure 4(b)). Summer weather in the Northern Hemisphere will reduce SARS-CoV-2 outdoor-lifetime significantly, potentially slowing the transmission of COVID-19. The predictions in Figure 3 are based on a constant temperature profile and do not account for daily temperature fluctuations, which may result in shorter lifetimes than predicted due to the exponential dependence of reaction rate on temperature. Additional environmental effects, like UV from sunlight, may further reduce inactivation time; with these limitations in mind, Figure 4 represents a conservative prediction of SARS-CoV-2 lifetime across the United States, and lifetimes greater than one month are not reported.

(a) Average Winter Temperatures, Jan-Mar 2020



(b) Average Summer Temperatures, Jul-Sep 2019



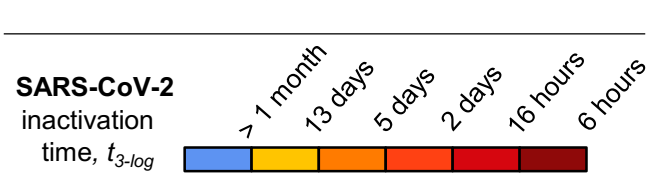


Figure 4 (Single Column). Lifetime of SARS-CoV-2 outside of a host across the United States in winter and summer. Predictions are based on (a) average temperature data from January to March, 2020 (corresponding to the onset of the COVID-19 pandemic), and (b) average temperature data from July to September, 2019 (to show characteristic lifetimes in summer). Temperatures are reported in Figures S34 and S35.

We tested the predictive ability of the thermodynamic model presented here by comparing the results to experimental data that had not been used to train the model. SARS-CoV-1 was reported to require 5 days

at room temperature to achieve a 5-log reduction;⁴⁶ our model predicts an inactivation time of 4.2 days under the same conditions. In another report, SARS-CoV-1 was heated to 56 °C and required only 6 minutes to achieve a 6-log reduction;²⁹ our model predicts a time of 17 minutes. A third report claimed that SARS-CoV-1 required 30 minutes to achieve an approximately 6-log reduction at 60 °C; ⁴⁷ our model predicts a time of 10 minutes. A more recent report shows that SARS-CoV-2 and SARS-CoV-1 both require 72 hours for a 3-log reduction on plastic surfaces maintained around 23 °C; our model predicts lifetimes of 80 hours and 50 hours, respectively, in good agreement with the reported data.³⁰ All of these reported lifetimes were within the uncertainty bounds of the model predictions. Considering the similarity in inactivation behavior for SARS-CoV-1 and SARS-CoV-2,³⁰ validation with SARS-CoV-1 suggests that this model will be a useful tool to estimate the lifetime of SARS-CoV-2.

The model is limited to temperature-based predictive ability and does not consider relative humidity or the fomite (i.e. the surface material on which a virion rests), both of which appear to affect inactivation times. 11,16,30,48 Variations in lifetime at a given temperature due to these environmental factors can be interpreted as catalytic effects; 49 incorporating a corresponding adjustment to the activation energy might enable additional predictive capabilities. Another limitation of this model is its reliance on a limited set of primary data which may contain experimental error (all primary data are reproduced in the supplementary material); statistical prediction uncertainties are described in the supplementary material, section S5. In addition, this model assumes that the enthalpy and entropy of the inactivation reaction are constant as temperature changes. This assumption is typically valid for macromolecules like proteins. 22 Some reports suggest multiple inactivation reaction pathways can occur near room temperature, but these reports are limited in scope do not agree with each other, and further work would need to be done before considering or implementing such effects. 31,40 Finally, the extrapolation of our model to higher temperatures outside the

range of the primary data (e.g. above 100 °C) may be unfounded if new inactivation reaction pathways become available at these elevated temperatures.

Fortunately, the results in **Table I** indicate that dry heat decontamination is feasible for inactivation of all types of coronaviruses, including SARS-CoV-2. The most common material used in surgical masks and N95 respirators is non-woven polypropylene, ^{50,51} which can be decontaminated with dry heat below its melting point (156 °C to 168 °C). ^{52,53} Cui and colleagues show that thermal cycling (75 °C, 30 min heating, applied over 20 cycles) does not degrade the filtration efficiency of N95-level facemasks, ⁹ and Lin, et al., report no significant degradation in the effectiveness of surgical masks after heating to 160 °C for 3 min. ⁷ Therefore, we expect that dry heat decontamination is an effective decontamination method, while also feasible within relatively short times (conservatively, less than 40 min at 70°C; **Table I**) and achievable by the majority of people with access to home ovens, rice cookers, or similar inexpensive heating devices.

In summary, this work provides guidelines to medical professionals and the general public for the effective, safe thermal decontamination of PPE. In addition, the sensitivity of coronaviruses to environmental temperature variations, shown in **Table I** and **Figure 4**, indicates that the thermal inactivation of SARS-CoV-2 must be considered in epidemiological studies predicting its global spread and, potentially, seasonal recurrence; our model can be incorporated into these studies due to its ability to predict virus lifetime as a continuous function of environmental temperature. Finally, the modeling framework presented here offers a new fundamental understanding of virus thermal inactivation that can help fight the COVID-19 pandemic as well as future outbreaks of other novel coronaviruses.

See the supplementary material for primary datasets for each virus studied in this work, tables of activation energy and frequency factor calculated from the data, temperature data in the United States corresponding to winter and summer, and details on the statistical analysis and uncertainty in predictions.

224

225

ACKNOWLEDGEMENTS

- We gratefully acknowledge helpful discussions with Dr. Dimithree Kahanda. This work was supported by
- 227 the National Science Foundation under grant CBET-2030023.

228 AUTHOR CONTRIBUTIONS

- 229 T.F.Y. and D.J.P. compiled and analyzed the data and developed the analytical model. All authors
- contributed to interpretation of results and writing and editing the manuscript. D.J.P. guided the work.

231 DATA AVAILABILITY

- The data that support the findings of this study are available within the article and its supplementary
- 233 material.

234

235

REFERENCES

- 236 (1) CDC COVID-19 Response Team. Characteristics of Health Care Personnel with COVID-19 —.
- 237 *MMWR Morb Mortal Wkly Rep.* **2020**, 69 (15), 477–481.
- 238 (2) Ranney, M. L.; Griffeth, V.; Jha, A. K. . Critical Supply Shortages The Need for Ventilators
- and Personal Protective Equipment during the Covid-19 Pandemic. N. Engl. J. Med. 2020, 41 (1),
- 240 1–3.
- Heimbuch, B. K.; Wallace, W. H.; Kinney, K.; Lumley, A. E.; Wu, C. Y.; Woo, M. H.; Wander, J.
- D. A Pandemic Influenza Preparedness Study: Use of Energetic Methods to Decontaminate
- Filtering Facepiece Respirators Contaminated with H1N1 Aerosols and Droplets. *Am. J. Infect.*

- 244 *Control* **2011**. https://doi.org/10.1016/j.ajic.2010.07.004.
- Viscusi, D. J.; King, W. P.; Shaffer, R. E. Effect of Decontamination on the Filtration Efficiency of Two Filtering Facepiece Respirator Models. *J. Int. Soc. Respir. Prot.* **2007**.
- 247 (5) Kolata, G. As Coronavirus Looms, Mask Shortage Gives Rise to Promising Approach. *The New York Times.* **2020**.
- 249 (6) Cramer, A.; Tian, E.; Yu, S. H.; Galanek, M.; Lamere, E.; Li, J.; Gupta, R.; Short, M. P.
- Disposable N95 Masks Pass Qualitative Fit-Test But Have Decreased Filtration Efficiency after
- 251 Cobalt-60 Gamma Irradiation. *medRxiv* **2020**. https://doi.org/10.1101/2020.03.28.20043471.
- 252 (7) Lin, T. H.; Tang, F. C.; Hung, P. C.; Hua, Z. C.; Lai, C. Y. Relative Survival of Bacillus Subtilis
- Spores Loaded on Filtering Facepiece Respirators after Five Decontamination Methods. *Indoor*
- 254 *Air* **2018**. https://doi.org/10.1111/ina.12475.
- Viscusi, D. J.; Bergman, M. S.; Eimer, B. C.; Shaffer, R. E. Evaluation of Five Decontamination
- 256 Methods for Filtering Facepiece Respirators. Ann. Occup. Hyg. 2009.
- 257 https://doi.org/10.1093/annhyg/mep070.
- 258 (9) Liao, L.; Xiao, W.; Zhao, M.; Yu, X.; Wang, H.; Wang, Q.; Chu, S.; Cui, Y. Can N95 Respirators
- Be Reused after Disinfection? How Many Times? ACS Nano 2020.
- 260 https://doi.org/10.1021/acsnano.0c03597.
- 261 (10) Xiang, Y.; Song, Q.; Gu, W. Decontamination of Surgical Face Masks and N95 Respirators by
- Dry Heat Pasteurization for One Hour at 70°C. Am. J. Infect. Control 2020, 000, 5–7.
- 263 https://doi.org/10.1016/j.ajic.2020.05.026.
- 264 (11) Chin, A. W. H.; Chu, J. T. S.; Perera, M. R. A.; Hui, K. P. Y.; Yen, H.-L.; Chan, M. C. W.; Peiris,
- 265 M.; Poon, L. L. M. Stability of SARS-CoV-2 in Different Environmental Conditions. *The Lancet*
- 266 *Microbe* **2020**. https://doi.org/10.1016/s2666-5247(20)30003-3.

- 267 (12) Lowen, A. C.; Steel, J. Roles of Humidity and Temperature in Shaping Influenza Seasonality. *J.*
- 268 *Virol.* **2014**. https://doi.org/10.1128/jvi.03544-13.
- 269 (13) Petrova, V. N.; Russell, C. A. The Evolution of Seasonal Influenza Viruses. *Nature Reviews*
- 270 *Microbiology*. **2018**. https://doi.org/10.1038/nrmicro.2017.118.
- 271 (14) Ikäheimo, T. M.; Jaakkola, K.; Jokelainen, J.; Saukkoriipi, A.; Roivainen, M.; Juvonen, R.;
- Vainio, O.; Jaakkola, J. J. K. A Decrease in Temperature and Humidity Precedes Human
- 273 Rhinovirus Infections in a Cold Climate. *Viruses* **2016**. https://doi.org/10.3390/v8090244.
- 274 (15) Sajadi, M. M.; Habibzadeh, P.; Vintzileos, A.; Miralles-wilhelm, F.; Amoroso, A. This Preprint
- 275 Research Paper Has Not Been Peer Reviewed. Electronic Copy Available at:
- 276 Https://Ssrn.Com/Abstract=3550308. **1992**, No. 410, 6–7.
- 277 (16) Casanova, L. M.; Jeon, S.; Rutala, W. A.; Weber, D. J.; Sobsey, M. D. Effects of Air Temperature
- and Relative Humidity on Coronavirus Survival on Surfaces. Appl. Environ. Microbiol. 2010.
- 279 https://doi.org/10.1128/AEM.02291-09.
- 280 (17) Rabenau, H. F.; Cinatl, J.; Morgenstern, B.; Bauer, G.; Preiser, W.; Doerr, H. W. Stability and
- Inactivation of SARS Coronavirus. Med. Microbiol. Immunol. 2005.
- https://doi.org/10.1007/s00430-004-0219-0.
- van Doremalen, N.; Bushmaker, T.; Munster, V. J. Stability of Middle East Respiratory Syndrome
- Coronavirus (MERS-CoV) under Different Environmental Conditions. Eurosurveillance 2013, 18
- 285 (38), 1–4. https://doi.org/10.2807/1560-7917.ES2013.18.38.20590.
- 286 (19) Leclercq, I.; Batéjat, C.; Burguière, A. M.; Manuguerra, J. C. Heat Inactivation of the Middle East
- Respiratory Syndrome Coronavirus. *Influenza Other Respi. Viruses* **2014**.
- 288 https://doi.org/10.1111/irv.12261.
- 289 (20) Kim, M. China finds heavy coronavirus traces in seafood, meat sections of Beijing food market

- 290 https://www.msn.com/en-gb/news/world/china-finds-heavy-coronavirus-traces-in-seafood-meat-
- sections-of-beijing-food-market/ar-BB15ETaQ?li=AAnZ9Ug (accessed Jun 23, **2020**).
- 292 (21) Lin, J.; Kang, M.; Zhong, H.; Zhang, X.; Yang, F.; Ni, H.; Huang, P.; Hong, T.; Ke, C.; He, J.
- Influenza Seasonality and Predominant Subtypes of Influenza Virus in Guangdong, China, 2004-
- 294 2012. J. Thorac. Dis. **2013**. https://doi.org/10.3978/j.issn.2072-1439.2013.08.09.
- 295 (22) Qin, Z.; Balasubramanian, S. K.; Wolkers, W. F.; Pearce, J. A.; Bischof, J. C. Correlated
- Parameter Fit of Arrhenius Model for Thermal Denaturation of Proteins and Cells. *Ann. Biomed.*
- *Eng.* **2014**. https://doi.org/10.1007/s10439-014-1100-y.
- 298 (23) U.S. FDA. Investigating Decontamination and Reuse of Respirators in Public Health
- 299 *Emergencies*; **2020**.
- 300 (24) FDA. Recommendations for Sponsors Requesting EUAs for Decontamination and Bioburden
- Reduction Systems for Face Masks and Respirators During the Coronavirus Disease 2019
- 302 (COVID-19) Public Health Emergency | FDA; 2020.
- 303 (25) CDC. Disinfection of Healthcare Equipment
- 304 https://www.cdc.gov/infectioncontrol/guidelines/disinfection/healthcare-equipment.html.
- 305 (26) CDC. Decontamination and Reuse of Filtering Facepiece Respirators Crisis Standards of Care
- Decontamination Recommendations Coronavirus Disease 2019 (COVID-19).
- 307 (27) Masters, P. S. The Molecular Biology of Coronaviruses. Advances in Virus Research. 2006.
- 308 https://doi.org/10.1016/S0065-3527(06)66005-3.
- 309 (28) Darnell, M. E. R.; Taylor, D. R. Evaluation of Inactivation Methods for Severe Acute Respiratory
- 310 Syndrome Coronavirus in Noncellular Blood Products. *Transfusion* **2006**.
- 311 https://doi.org/10.1111/j.1537-2995.2006.00976.x.
- 312 (29) Kariwa, H.; Fujii, N.; Takashima, I. Inactivation of SARS Coronavirus by Means of Povidone-

- Iodine, Physical Conditions and Chemical Reagents. In *Dermatology*; **2006**.
- https://doi.org/10.1159/000089211.
- van Doremalen, N.; Bushmaker, T.; Morris, D. H.; Holbrook, M. G.; Gamble, A.; Williamson, B.
- N.; Tamin, A.; Harcourt, J. L.; Thornburg, N. J.; Gerber, S. I.; Lloyd-Smith, J. O.; de Wit, E.;
- Munster, V. J. Aerosol and Surface Stability of SARS-CoV-2 as Compared with SARS-CoV-1. *N*.
- 318 Engl. J. Med. **2020**. https://doi.org/10.1056/nejmc2004973.
- 319 (31) Laude, H. Thermal Inactivation Studies of a Coronavirus, Transmissible Gastroenteritis Virus. J.
- 320 Gen. Virol. 1981. https://doi.org/10.1099/0022-1317-56-2-235.
- 321 (32) Lelie, P. N.; Reesink, H. W.; Lucas, C. J. Inactivation of 12 Viruses by Heating Steps Applied
- during Manufacture of a Hepatitis B Vaccine. *J. Med. Virol.* **1987**.
- 323 https://doi.org/10.1002/jmv.1890230313.
- 324 (33) Saknimit, M.; Inatsuki, I.; Sugiyama, Y.; Yagami, K. Virucidal Efficacy of Physico-Chemical
- Treatments against Coronaviruses and Parvoviruses of Laboratory Animals. *Jikken Dobutsu.* **1988**.
- 326 https://doi.org/10.1538/expanim1978.37.3 341.
- 327 (34) Quist-Rybachuk, G. V.; Nauwynck, H. J.; Kalmar, I. D. Sensitivity of Porcine Epidemic Diarrhea
- Virus (PEDV) to PH and Heat Treatment in the Presence or Absence of Porcine Plasma. *Vet.*
- 329 *Microbiol.* **2015**. https://doi.org/10.1016/j.vetmic.2015.10.010.
- 330 (35) C.R., S. Thermobacteriology in Food Processing (2nd Ed). New York Acad. Press 1973.
- 331 (36) Xiong, R.; Xie, G.; Edmondson, A. E.; Sheard, M. A. A Mathematical Model for Bacterial
- 332 Inactivation. Int. J. Food Microbiol. 1999. https://doi.org/10.1016/S0168-1605(98)00172-X.
- 333 (37) CERF, O. A REVIEW Tailing of Survival Curves of Bacterial Spores. J. Appl. Bacteriol. 1977.
- https://doi.org/10.1111/j.1365-2672.1977.tb00665.x.
- 335 (38) Casolari, A. Microbial Death. In *Physiological Models in Microbiology: Volume II*; **2018**.

- https://doi.org/10.1201/9781351075640.
- 337 (39) Van Boekel, M. A. J. S. On the Use of the Weibull Model to Describe Thermal Inactivation of
- Microbial Vegetative Cells. *Int. J. Food Microbiol.* **2002**. https://doi.org/10.1016/S0168-
- 339 1605(01)00742-5.
- 340 (40) Price, W. C. Thermal Inactivation Rates of Four Plant Viruses. Arch. Gesamte Virusforsch. 1940.
- 341 https://doi.org/10.1007/BF01245548.
- 342 (41) Wright, N. T. On a Relationship between the Arrhenius Parameters from Thermal Damage
- 343 Studies. J. Biomech. Eng. 2003. https://doi.org/10.1115/1.1553974.
- 344 (42) Rutala, W. A.; Weber, D. J. Low-Temperature Sterilization Technologies: Do We Need to
- Redefine "Sterilization"? *Infect. Control Hosp. Epidemiol.* **1996**.
- https://doi.org/10.2307/30141007.
- Oral, E.; Wannomae, K. K.; Connolly, R.; Gardecki, J.; Leung, H. M.; Muratoglu, O.; Griffiths,
- 348 A.; Honko, A. N.; Avena, L. E.; Mckay, L. G. A.; Flynn, N.; Storm, N.; Downs, S. N.; Jones, R.;
- Emmal, B. Vapor H 2 O 2 Sterilization as a Decontamination Method for the Reuse of N95
- Respirators in the COVID-19 Emergency. **2020**, *4* (596), 1–5.
- https://doi.org/10.1101/2020.04.11.20062026.
- 352 (44) Yeo, C.; Kaushal, S.; Yeo, D. Enteric Involvement of Coronaviruses: Is Faecal–Oral Transmission
- of SARS-CoV-2 Possible? Lancet Gastroenterol. Hepatol. 2020, 5 (4), 335–337.
- https://doi.org/10.1016/S2468-1253(20)30048-0.
- 355 (45) Firquet, S.; Beaujard, S.; Lobert, P. E.; Sané, F.; Caloone, D.; Izard, D.; Hober, D. Survival of
- Enveloped and Non-Enveloped Viruses on Inanimate Surfaces. *Microbes Environ.* **2015**, *30* (2),
- 357 140–144. https://doi.org/10.1264/jsme2.ME14145.
- 358 (46) Lai, M. Y. Y.; Cheng, P. K. C.; Lim, W. W. L. Survival of Severe Acute Respiratory Syndrome

- 359 Coronavirus. *Clin. Infect. Dis.* **2005**. https://doi.org/10.1086/433186.
- 360 (47) Yunoki, M.; Urayama, T.; Yamamoto, I.; Abe, S.; Ikuta, K. Heat Sensitivity of a SARS-
- Associated Coronavirus Introduced into Plasma Products. *Vox Sang.* **2004**.
- 362 https://doi.org/10.1111/j.1423-0410.2004.00577.x.
- 363 (48) Chan, K. H.; Peiris, J. S. M.; Lam, S. Y.; Poon, L. L. M.; Yuen, K. Y.; Seto, W. H. The Effects of
- Temperature and Relative Humidity on the Viability of the SARS Coronavirus. *Adv. Virol.* **2011**.
- 365 https://doi.org/10.1155/2011/734690.
- 366 (49) Roduner, E. Understanding Catalysis. *Chemical Society Reviews*. **2014**.
- 367 https://doi.org/10.1039/c4cs00210e.
- 368 (50) Bałazy, A.; Toivola, M.; Adhikari, A.; Sivasubramani, S. K.; Reponen, T.; Grinshpun, S. A. Do
- N95 Respirators Provide 95% Protection Level against Airborne Viruses, and How Adequate Are
- 370 Surgical Masks? *Am. J. Infect. Control* **2006**, *34* (2), 51–57.
- 371 https://doi.org/10.1016/j.ajic.2005.08.018.
- 372 (51) Belkin, N. L. The Surgical Mask: Are New Tests Relevant for OR Practice? AORN J. 2009, 89 (5),
- 373 883–891. https://doi.org/10.1016/j.aorn.2008.09.016.
- 374 (52) Tiganis, B. E.; Shanks, R. A.; Long, Y. Effects of Processing on the Microstructure, Melting
- Behavior, and Equilibrium Melting Temperature of Polypropylene. J. Appl. Polym. Sci. 1996, 59
- 376 (4), 663–671. https://doi.org/10.1002/(sici)1097-4628(19960124)59:4<663::aid-app12>3.3.co;2-c.
- 377 (53) Duran, K.; Duran, D.; Oymak, G.; Kiliç, K.; Öncü, E.; Kara, M. Investigation of the Physical
- Properties of Meltblown Nonwovens for Air Filtration. *Tekst. ve Konfeksiyon* **2013**, *23* (2), 136–
- 379 142.
- 380 (54) Possee, R. D. Baculovirus Expression Vectors A Laboratory Manual. *Trends Biotechnol.* **1993**.
- 381 https://doi.org/10.1016/0167-7799(93)90146-z.

- Neill, K. O.; Huang, N.; Unis, D.; Clem, R. J. Rapid Selection against Arbovirus-Induced
 Apoptosis during Infection of a Mosquito Vector. *Proc. Natl. Acad. Sci. U. S. A.* **2015**.

 https://doi.org/10.1073/pnas.1424469112.
- Li, S.; Zhao, H.; Yang, H.; Hou, W.; Cruz-Cosme, R.; Cao, R.; Chen, C.; Wang, W.; Xu, L.;
 Zhang, J.; Zhong, W.; Xia, N.; Tang, Q.; Cheng, T. Rapid Neutralization Testing System for Zika
 Virus Based on an Enzyme-Linked Immunospot Assay. *ACS Infect. Dis.* 2020.
 https://doi.org/10.1021/acsinfecdis.9b00333.
- Montgomery, D. C.; Runger, G. C. *Applied Statistics and Probability for Engineers*, 3rd ed.; John Wiley & Sons, Inc, **2003**. https://doi.org/10.1080/03043799408928333.